Transport properties of carbon nanotubes encapsulating C_{60} and related materials

Hisashi Kondo
Institute of Industrial Science, University of Tokyo, 4-6-1 Komaba, Meguro-ku, Tokyo 153-8505, Japan
and Computational Materials Science Center, National Institute for Materials Science (NIMS), 1-2-1 Sengen, Tsukuba, Ibaraki 305-0047, Japan

Hiori Kino
Computational Materials Science Center, National Institute for Materials Science (NIMS), 1-2-1 Sengen, Tsukuba, Ibaraki 305-0047, Japan

Takahisa Ohno
Computational Materials Science Center, National Institute for Materials Science (NIMS), 1-2-1 Sengen, Tsukuba, Ibaraki 305-0047, Japan
and Institute of Industrial Science, University of Tokyo, 4-6-1 Komaba, Meguro-ku, Tokyo 153-8505, Japan
(Received 28 May 2004; revised manuscript received 27 October 2004; published 14 March 2005)

We have investigated the transport properties of various periodic and nonperiodic $C_{60}@(10,10)$ peapod systems by varying the distribution of C_{60}s encapsulated in the (10,10) nanotube, based on Green function approach within the realistic tight-binding model. The transport properties of the $C_{60}@(10,10)$ systems strongly depend on the distribution of the C_{60}s encapsulated in the (10,10) nanotube. The periodic systems exhibit the quantized transmissions reflecting their band structure. The transmission of the system with a C_{120} molecule in an infinite array of C_{60}s has dip structures around the energy levels of the C_{120} molecule, the half widths of which are dependent on the strength of the interaction between the nanotube and the impurity C_{120} molecule.

DOI: 10.1103/PhysRevB.71.115413 PACS number(s): 73.63.Fg, 72.80.Rj

I. INTRODUCTION

Carbon nanotubes[1] have attracted great attention because of their potential application to electronic nano-devices utilizing the multiplicity of transport property due to their topological structures.[2–4] In the silicon device technologies, carrier doping by introducing impurities is one of the fundamental techniques to modify the transport properties of silicon-based materials drastically. The possibility of the carrier doping into carbon nanotubes has been investigated recently, and it is reported that their electronic and transport properties are significantly altered by materials encapsulated in them. For example, zigzag nanotubes, which are insulating by nature, are predicted to be metallic when they encapsulate alkali atoms such as potassium; there exist states related to the alkali atoms at the Fermi energy.[5] Another interesting example is a peapod, which is a single-wall carbon nanotube encapsulating an array of fullerene molecules inside.[6,7] First-principles calculations have shown that a (10,10) nanotube encapsulating C_{60}s periodically [denoted by $C_{60}@(10,10)$], which is called a periodic peapod, exhibits a metallic character with multicarriers.[8] A nanotube encapsulating larger fullerenes, that is, $C_{78}@(11,11)$ is also reported to have a metallic character with multicarriers.[9] In this way, the carbon nanotube system encapsulating fullerene molecules is a good candidate for application to electronic nano-devices.

In the present study we investigate the transport properties of various periodic and nonperiodic $C_{60}@(10,10)$ peapod systems by varying the distribution of C_{60}s inside the (10,10) nanotube. In addition, we examine the peapod system with one C_{120} molecule, such as a C_{60} dimer, a peanut, and a (5,5) capsule[10] as an impurity in an infinite array of C_{60}s. For this purpose, we employ the Green function approach[11] within a realistic tight-binding model. Some transport calculations have been reported for the nanotubes encapsulating a few C_{60}s.[12,13] Our target is the nanotubes encapsulating infinite fullerenes, instead. We especially focus on the effects of the fullerene distribution and of the C_{60}-related defect structures on the transport properties.

II. MODEL AND APPROACH

In the present work, we use a realistic tight-binding model taking account of carbon 2*s* and 2*p* atomic orbitals.[3,14] Transfer integrals are carefully prepared to reproduce well the band structure of graphite obtained by the all-electron full-potential linearized augmented plane wave method. In addition, this model can reproduce well the band structure of carbon nanotubes obtained by the first-principles calculation, except the nearly free electron (NFE) state. This NFE state corresponds to the interlayer state in graphite. This interlayer state has very small amplitude in the atomic region. For the periodic $C_{60}@(10,10)$ peapod, the atomic levels for the carbon atoms which belong to C_{60} are shifted down by 0.75 eV in the tight-binding parameter set,[15] in order to reproduce well the band structure of $C_{60}@(10,10)$ obtained by the first-principles calculation,[8] as shown in Fig. 2(a). This atomic level shift is reasonable because the effect of hybridization between the NFE state and the states of C_{60} is not taken into account in the original tight-binding model includ-

ing 2*s* and 2*p* orbitals. We assume the same atomic level shift when the structures of encapsulated C_{60} change. In addition, we set the diameter of (10,10) nanotube and C_{60} to be 6.75 and 3.32 Å, respectively, and geometry optimizations are not carried out.

We study the transport properties of the systems connecting with semi-infinite electrodes. For convenience we separate the system into three parts: (a) semi-infinite left lead (left region), (b) central (interaction) region and (c) semi-infinite right lead (right region). Then, the Hamiltonian matrix is given by

$$\mathcal{H} = \begin{pmatrix} H_{\mathrm{L}} & H_{\mathrm{LC}} & 0 \\ H_{\mathrm{CL}} & H_{\mathrm{C}} & H_{\mathrm{CR}} \\ 0 & H_{\mathrm{RC}} & H_{\mathrm{R}} \end{pmatrix}, \tag{1}$$

where we assume that there is no interaction between the left and right region. The overlap matrix $\mathcal{S}$ is written in the same form as Eq. (1)

$$\mathcal{S} = \begin{pmatrix} S_{\mathrm{L}} & S_{\mathrm{LC}} & 0 \\ S_{\mathrm{CL}} & S_{\mathrm{C}} & S_{\mathrm{CR}} \\ 0 & S_{\mathrm{RC}} & S_{\mathrm{R}} \end{pmatrix}. \tag{2}$$

Green function $\mathcal{G}(z)$ is defined by

$$(z\mathcal{S} - \mathcal{H})\mathcal{G}(z) = \mathcal{I}, \tag{3}$$

where z and $\mathcal{I}$ are an arbitrarily complex number and the unit matrix, respectively. Then, the Green function at central region is calculated as

$$G_{\mathrm{C}}(z) = [zS_{\mathrm{C}} - H_{\mathrm{C}} - \Sigma_{\mathrm{L}}(z) - \Sigma_{\mathrm{R}}(z)]^{-1}, \tag{4}$$

where

$$\Sigma_{\mathrm{L}}(z) = (zS_{\mathrm{CL}} - H_{\mathrm{CL}})G_{\mathrm{L}}(z)(zS_{\mathrm{LC}} - H_{\mathrm{LC}}), \tag{5}$$

$$\Sigma_{\mathrm{R}}(z) = (zS_{\mathrm{CR}} - H_{\mathrm{CR}})G_{\mathrm{R}}(z)(zS_{\mathrm{RC}} - H_{\mathrm{RC}}), \tag{6}$$

where $G_{\mathrm{L/R}}(z) = (zS_{\mathrm{L/R}} - H_{\mathrm{L/R}})^{-1}$ is the surface Green function for the left/right region and we calculate the matrix elements for the layers neighboring the central region.[16]

The transmission is evaluated as

$$T(\varepsilon) = \mathrm{Tr}[\Gamma_{\mathrm{L}}(\varepsilon)G_{\mathrm{C}}^{r}(\varepsilon)\Gamma_{\mathrm{R}}(\varepsilon)G_{\mathrm{C}}^{a}(\varepsilon)], \tag{7}$$

where

$$\Gamma_{\mathrm{L}}(\varepsilon) = \mathrm{i}[\Sigma_{\mathrm{L}}^{r}(\varepsilon) - \Sigma_{\mathrm{L}}^{a}(\varepsilon)], \tag{8}$$

$$\Gamma_{\mathrm{R}}(\varepsilon) = \mathrm{i}[\Sigma_{\mathrm{R}}^{r}(\varepsilon) - \Sigma_{\mathrm{R}}^{a}(\varepsilon)], \tag{9}$$

where $G_{\mathrm{C}}^{r}(\varepsilon) = G_{\mathrm{C}}(\varepsilon + 0^{+})$ $[G_{\mathrm{C}}^{a}(\varepsilon) = G_{\mathrm{C}}(\varepsilon - 0^{+})]$ and $\Sigma_{\mathrm{L/R}}^{r}(\varepsilon) = \Sigma_{\mathrm{L/R}}(\varepsilon + 0^{+})$ $[\Sigma_{\mathrm{L/R}}^{a}(\varepsilon) = \Sigma_{\mathrm{L/R}}(\varepsilon - 0^{+})]$ are the retarded (advanced) Green function for the central region and the retarded (advanced) self-energy of the left/right region, respectively. In the present work, we calculate the energy dependence of the transmission function under zero source-drain voltage.

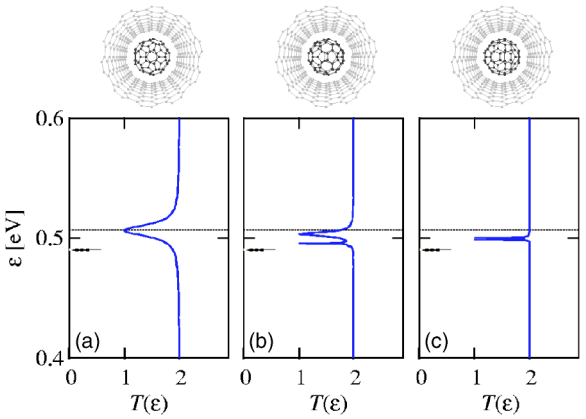

FIG. 1. The transmissions and atomic structures of the (10,10) nanotube with one C_{60} in the central region. The encapsulated C_{60} is rotated by angle θ on the one perpendicular axis to the tube axis. (a) $\theta = 0°$, (b) 12° and (c) 24°. Arrows show the energy levels of t_{1u} state of C_{60}.

III. RESULTS AND DISCUSSIONS

A. System encapsulating only one C_{60}

To begin with, we calculate the transmission of the (10,10) nanotube encapsulating only one C_{60} molecule $[1C_{60}@(10,10)]$, as shown in Fig. 1. The C_{60} molecule has the threefold degenerated t_{1u} state at 0.490 eV, which is close to the Fermi level of the (10,10) nanotube. The degenerated t_{1u} state is characterized by the quantum number $m = -1$, 0 and +1.[17–19] How the t_{1u} state of C_{60} affects the transport properties of the (10,10) nanotube is of interest. Here it is noted that the (10,10) nanotube exhibits a metallic character with the calculated transmission $T(\varepsilon) = 2$ around the Fermi energy. We consider three configurations of C_{60} by changing the rotation angle θ with respect to one of the molecular axes perpendicular to the tube axis. At $\theta = 0°$, the calculated transmission $T(\varepsilon)$ has one broad dip around the t_{1u} state of C_{60}, and $T(\varepsilon) = 1$ at the bottom of the dip. In the case of $\theta = 0°$, where a fivefold rotational symmetry axis of C_{60} coincides with the (10,10) nanotube axis, the system has both mirror and rotational symmetries. As a result, the t_{1u} state of C_{60} characterized by $m = 0$ is coupled with the state of the (10,10) nanotube and acts as a scattering center, which leads to the appearance of one dip in the transmission $T(\varepsilon)$. With increasing θ, the half width of the dip decreases and the dip shifts closer to the t_{1u} state of C_{60}. At $\theta \neq 0°$, all of the t_{1u} states of C_{60} become coupled with the nanotube state because of the symmetry breaking of the system and, as a result, the transmission has another dip. Namely, the calculated transmission has two dips and $T(\varepsilon) = 1$ at the bottoms of both dips; one dip at a higher energy is related to the $m = 0$ state of the t_{1u} state of C_{60} and another at a lower energy is related to the $m = -1$ and +1 states.

The results of the transmission of $1C_{60}@(10,10)$ are well understood by a simple one-dimensional model, which is given in Appendix A. The simple model suggests that both the position and the half width of the dip in the transmission depend on the strength of the interaction between (10,10) nanotube and C_{60} [see Appendix A]. At $\theta = 0°$, the broad dip

appears considerably away from the t_{1u} state of C_{60}. This indicates that the interaction between (10,10) nanotube and C_{60} is strong. At $\theta \neq 0°$, on the other hand, the interaction between (10,10) nanotube and C_{60} seems weaker, which results in the narrower dip closer to the t_{1u} state of C_{60}. Consequently, C_{60} merely acts as a scattering impurity center when introduced in the (10,10) nanotube.

For the $1C_{60}@(10,10)$ system, it is reported from first-principles calculations that the t_{1u} state of C_{60} is located just above the Fermi energy,[20] while the t_{1u} state is located just below the Fermi energy in our tight-binding calculations. In the present study, the atomic levels for the carbon atoms which belong to C_{60} are shifted down by 0.75 eV in the tight-binding parameter set and the same atomic level shift is assumed for the $1C_{60}@(10,10)$ system. If we calculated the electronic structure in a self-consistent manner, a large amount of charge transfer would occur between the nanotube and the C_{60}, which would induce significant long-range Coulomb interactions between them. Our non-self-consistent tight-binding calculations do not take into account such charge transfer and long-range interactions. The first-principles result showing the negligible charge transfer also indicates that there are no such long-range interactions. Thus, we think that our tight-binding parameter set reproduces the electronic structure of the $1C_{60}@(10,10)$ system fairly well, except for the precise position of the t_{1u} state of C_{60} relative to the Fermi energy. This implies that the effect of the t_{1u} state of C_{60} on the transport properties, such as resonant scattering, may be qualitatively well described in terms of non-self-consistent calculations, except for the exact resonance position.

B. System with infinite C_{60}s

Here, we study the transport properties of the periodic $C_{60}@(10,10)$ peapod, as shown in Fig. 2(a). The distance between centers of neighboring encapsulated C_{60}s, which corresponds to the lattice constant along the tube direction ℓ_0, is 9.845 Å. Figure 2(b) presents the transmission $T(\varepsilon)$ and the band structure of the $C_{60}@(10,10)$, and the magnifications of them around the Fermi energy ε_F are also shown in Fig. 2(c). Besides the bands coming from the (10,10) nanotube, there exist two narrow bands near the Fermi energy; one is the band originated from the t_{1u} state of C_{60} characterized by $m=0$ while the other is the twofold degenerated band from the t_{1u} states characterized by $m=-1$ and +1. Since a fivefold rotational symmetry axis of C_{60} coincides with the (10,10) nanotube axis, this peapod system has both mirror and rotational symmetries. As a result, the band from t_{1u} state with $m=0$ is coupled with the nanotube bands, whereas the twofold degenerated band from the t_{1u} states with $m=-1$ and +1 is not. The Fermi level is found to cross the degenerated band near the Γ point, and then the transmission at the Fermi energy ε_F has contributions both from the (10,10) nanotube and from the t_{1u} states with $m=-1$ and +1, having $T(\varepsilon_F)=4$. This means that the periodic $C_{60}@(10,10)$ exhibits transport properties with multicarriers; the electrons both in the (10,10) nanotube and in the array of C_{60}s are transmitted. On the other hand, around 0.46 and 0.54 eV

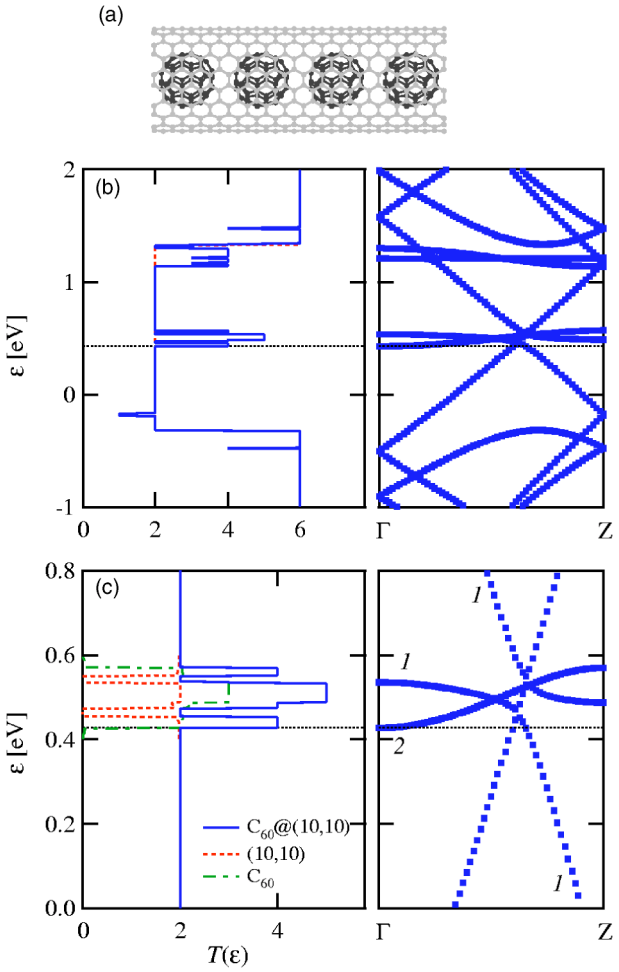

FIG. 2. (a) Atomic structure of the periodic $C_{60}@(10,10)$. (b) The transmission (left) and the band structure (right) of periodic $C_{60}@(10,10)$, where the distance between encapsulated C_{60}, or the lattice constant, is 9.845 Å. (c) The transmission and the band structure of the same system around Fermi energy. In (c), dashed and dashed-dotted lines show contributions to the transmission from (10,10) nanotube and C_{60}, respectively. Dotted lines show Fermi energies.

where the bands from the nanotube and from the t_{1u} state with $m=0$ are missing due to the band repulsion between them, the transmission arises only from the twofold degenerated band of the t_{1u} states with $m=-1$ and +1. At the energy range of about 0.49–0.53 eV, the band from the t_{1u} state with $m=0$ also makes a contribution to the transmission. In this way, the transport properties reflect well the band structure because the $C_{60}@(10,10)$ is a periodic system.

We consider other periodic $C_{60}@(10,10)$ systems with larger lattice constants ℓ_0 of 12.306 and 14.768 Å, as well. In these systems, C_{60}s are located at positions commensurate with the (10,10) nanotube. There is no direct interaction between neighboring C_{60}s, since the distance between them is larger than the cutoff radius of 4.0 Å in the tight-binding model. The transmission $T(\varepsilon)$ and the band structure of these systems are shown in Fig. 3. Since there is no state at the Fermi energy because of band repulsion, the $C_{60}@(10,10)$s

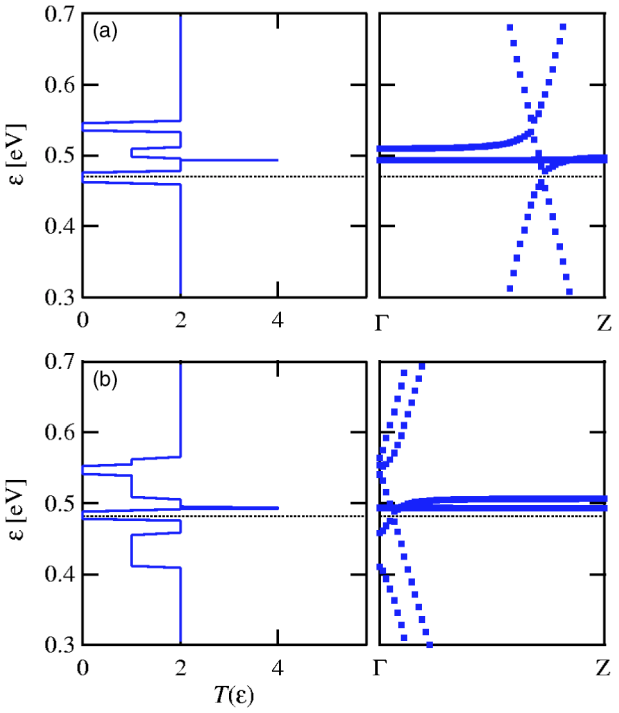

FIG. 3. The transmissions and band structures of the periodic C_{60}@(10,10). The distances between the encapsulated C_{60}, or the lattice constants, are 12.306 Å in (a) and 14.768 Å in (b).

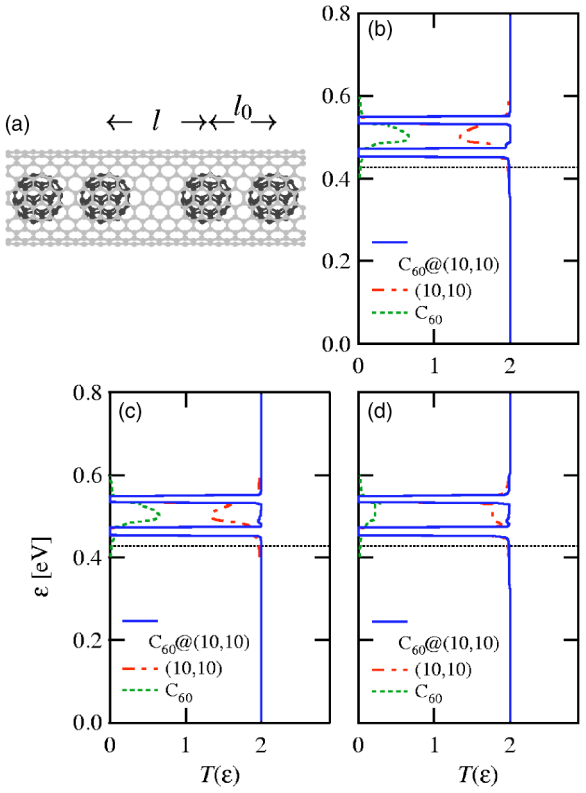

FIG. 4. (a) Atomic structure of the nonperiodic C_{60}@(10,10) with ℓ_0 and ℓ, where ℓ and ℓ_0 are the distance between centers of two C_{60}s at central region and lattice constant of the left and right electrode, respectively. The transmission of the (10,10) nanotube encapsulating C_{60}s with ℓ_0=9.845 Å and (b) ℓ=12.036 Å, (c) 14.767 Å and (d) 29.535 Å. Dashed and dashed-dotted lines show contributions to the transmission from C_{60} and the (10,10) nanotube, respectively. Dashed line shows Fermi energy of electrode.

with these large lattice constants are insulators. The transmission arises only from contribution through the (10,10) nanotube, except that the t_{1u} states of C_{60} make a contribution in a very narrow range around 0.493 eV. Thus, the C_{60}@(10,10)s with large lattice constants ($\ell_0 > 10.64$ Å) do not exhibit transport properties with multicarriers.

Next we examine the transport properties of nonperiodic C_{60}@(10,10). We introduce a nonperiodicity to the C_{60}@(10,10) systems with ℓ_0=9.845 Å, by changing the distance ℓ between centers of two C_{60}s at the central region from ℓ_0, as shown in Fig. 4(a). If we choose $\ell > 10.64$ Å, the matrix elements of the Hamiltonian between the two central C_{60}s equal zero. Figures 4(b)–4(d) present the transmission $T(\varepsilon)$ of the C_{60}@(10,10) systems with ℓ_0=9.845 Å and ℓ =12.036, 14.767, and 29.535 Å. It is noteworthy that the total transmission of these nonperiodic systems is independent of ℓ. The total transmissions are the same as the contribution from the (10,10) nanotube in the transmission of the pristine C_{60}@(10,10), which corresponds to the dashed line in Fig. 2(c). The transmission at the Fermi energy ε_F, $T(\varepsilon_F)$, equals ~2.

At the energy range of 0.4–0.6 eV, the transmission through the (10,10) nanotube of the nonperiodic C_{60}@(10,10) system has a dip structure because of the nonperiodic arrangement of encapsulating C_{60}s. This situation is similar to the (10,10) nanotube with an impurity molecule [see Appendix A]. The electrons of the (10,10) nanotube are scattered by the nonperiodicity of the C_{60} array in the central region. Therefore, the dip structure appears around the t_{1u} states of C_{60}. The dip depth decreases with increasing ℓ, which indicates that the states in the left and the right regions are more smoothly connected in the central region when ℓ becomes larger. Surprisingly, at the same energy range of 0.4–0.6 eV, the transmission has some contribution from C_{60}. Since there is no direct interaction between the two central C_{60}s, the contribution from C_{60} probably arises from the connection between the states of C_{60}s in the electrodes and those of the (10,10) nanotube in the central region. In addition, these systems have no state of the (10,10) nanotube around both 0.46 and 0.54 eV. This is because of the level repulsion between the (10,10) nanotube and the C_{60}s, which is independent of the distribution of C_{60}.

We consider this type of nonperiodic C_{60}@(10,10) system with larger lattice constants of ℓ_0=12.306 and 14.768 Å, as well. It is found from Fig. 5 that the transmissions of these nonperiodic systems with $\ell_0 > 10.64$ Å are smaller than that of the periodic system with $\ell = \ell_0$. The transmission of the periodic system has a contribution only from (10,10) nanotube since there is no direct interaction between neighboring C_{60}s in the electrodes. These results are in contrast with the case of ℓ_0=9.845 Å showing that the transmission of the nonperiodic system is the same as the contribution from the (10,10) nanotube in the transmission of the periodic system. When $\ell_0 > 10.64$ Å, there is no contribution from C_{60} which could compensate the scattering of the (10,10) nanotube

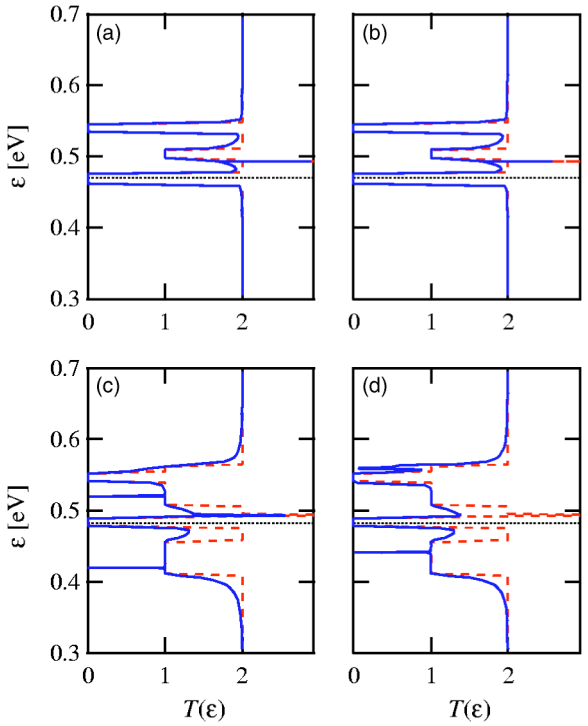

FIG. 5. The transmission of the nonperiodic C_{60}@(10,10)s whose atomic structures are shown in Fig. 4(a), with (a) ℓ =17.229 Å and ℓ_0=12.306 Å, (b) ℓ=22.151 Å and ℓ_0=12.306 Å, (c) ℓ=19.690 Å and ℓ_0=14.768 Å and (d) ℓ=24.613 Å and ℓ_0 =14.768 Å, where ℓ and ℓ_0 are the distance between centers of two C_{60}s at the central region and lattice constant of the left and right electrode, respectively. Dashed and dotted line show the transmission of the pristine C_{60}@(10,10) with ℓ_0 and Fermi energy of electrode, respectively.

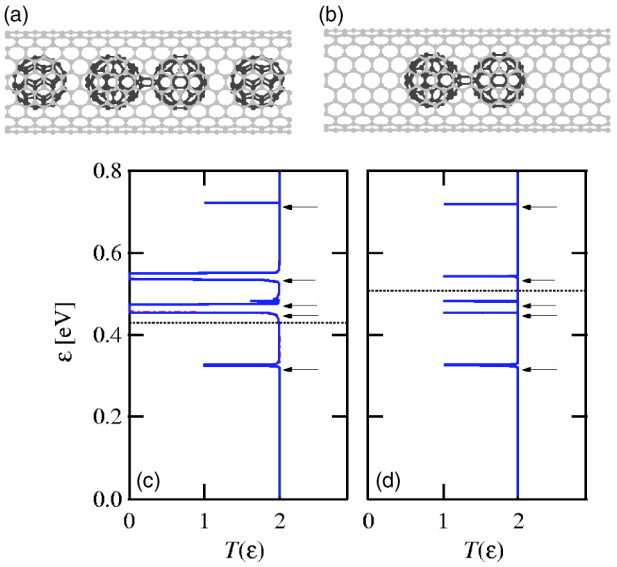

FIG. 6. (a) Atomic structure of the C_{60}@(10,10) with C_{60} dimer. (b) Atomic structure of the (10,10) nanotube encapsulating only C_{60} dimer without C_{60}s. (c) The transmission of C_{60}@(10,10) with C_{60} dimer. Dotted-dashed lines show the transmission of C_{60}@(10,10) with ℓ_0=9.845 Å and ℓ=29.535 Å. (d) The transmission of C_{60}@(10,10) encapsulating only C_{60} dimer without C_{60}. Arrows show energy levels of the C_{60} dimer. Dotted lines show the Fermi energies of electrodes.

states due to the nonperiodicity of the C_{60} array.

It is known that C_{60}s are polymerized into C_{120} molecules such as C_{60} dimers, peanuts and (5,5) capsules.[10] We assume that two C_{60}s in the central region of the periodic C_{60}@(10,10) with ℓ_0=9.845 Å [Fig. 2(a)] are transformed into a C_{120} molecule. The obtained C_{60}@(10,10) with the C_{120} molecule is also regarded as a system where the C_{120} molecule is introduced as an impurity into the nonperiodic C_{60}@(10,10) with ℓ_0=9.845 Å and ℓ=29.535 Å [Fig. 4(d)]. Here, we study the transport properties of C_{60}@(10,10) with a C_{60} dimer, a peanut, and a (5,5) capsule as C_{120} molecule in the central region. In these C_{60}@(10,10) systems with the C_{120} molecule, we assume that C_{60}s are located at positions commensurate with the (10,10) nanotube and that the distance between the C_{120} molecule and the left-side C_{60} is the same as that between neighboring C_{60}s in the pristine periodic C_{60}@(10,10).

For the C_{60}@(10,10) with the C_{60} dimer, which is shown in Fig. 6(a), the distance between the C_{60} dimer and the right-side C_{60} (the left-side C_{60}) is 3.629 Å (3.203 Å). This indicates that the interaction between the C_{60} dimer and the right-side C_{60} is weak. Figure 6(c) shows the transmission $T(\varepsilon)$ of this system, together with the energy levels of the C_{60} dimer. The transmission has narrow dips around the energy levels of the C_{60} dimer and $T(\varepsilon)\sim 1$ at the bottom of each dip, except the dip around 0.470 eV. This is probably because the transmission around 0.470 eV includes a contribution through encapsulated C_{60} molecules. Except for the dip structure, the transmission is the same as that in the C_{60}@(10,10) system with ℓ_0=9.845 Å and ℓ=29.535 Å without including the C_{60} dimer, which is shown in Fig. 4(d). Furthermore, the dip features at 0.315 and 0.712 eV are the same as those of the (10,10) nanotube encapsulating only the C_{60} dimer without the left/right arrays of C_{60}s [Fig. 6(b)], as shown in Fig. 6(d). This result suggests that the electronic states of the C_{60} dimer weakly interact with the (10,10) nanotube states, as discussed in Appendix A. Thus, the C_{60} dimer merely acts as a scattering impurity center when introduced in the nonperiodic C_{60}@(10,10) without the C_{60} dimer.

For the C_{60}@(10,10) with the peanut, the distance between the peanut and the right-side C_{60} (the left-side C_{60}) is 4.461 Å (3.203 Å) [Fig. 7(a)]. This means that the peanut does not interact with the right side, but with the left-side C_{60}. The transmission of the C_{60}@(10,10) with the peanut and that of the (10,10) nanotube encapsulating only the peanut without C_{60}s [Fig. 7(b)] are shown in Figs. 7(c) and 7(d), respectively, together with the energy levels of the peanut. The transmission has dips around the levels of the peanut. Thus the C_{60}@(10,10) with the peanut exhibits qualitatively the same features as the C_{60}@(10,10) with the C_{60} dimer.

The transmission of the C_{60}@(10,10) with the (5,5) capsule [Fig. 8(a)] together with the energy levels of the (5,5) capsule are shown in Fig. 8(c). The distance between the (5,5) capsule and the right-side C_{60} (the left-side C_{60}) is 5.740 Å (3.278 Å). Namely, the (5,5) capsule does not interact with the right side, but with the left-side C_{60}. We find no

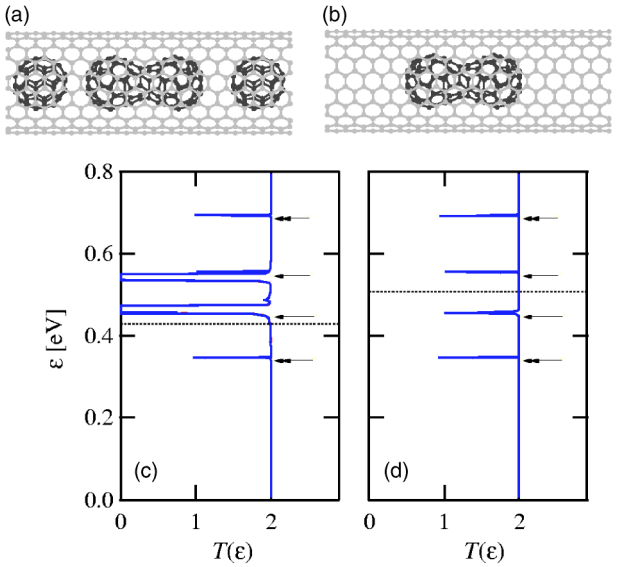

FIG. 7. (a) Atomic structure of the the C_{60}@(10,10) with the peanut. (b) Atomic structure of the (10,10) nanotube encapsulating only peanut without C_{60}s. (c) The transmission of C_{60}@(10,10) with the peanut. Dotted-dashed lines show the transmission of C_{60}@(10,10) with ℓ_0=9.845 Å and ℓ=29.535 Å. (d) The transmission of C_{60}@(10,10) encapsulating only peanut without C_{60}. Arrows show energy levels of the peanut. Dotted lines show the Fermi energies of electrodes.

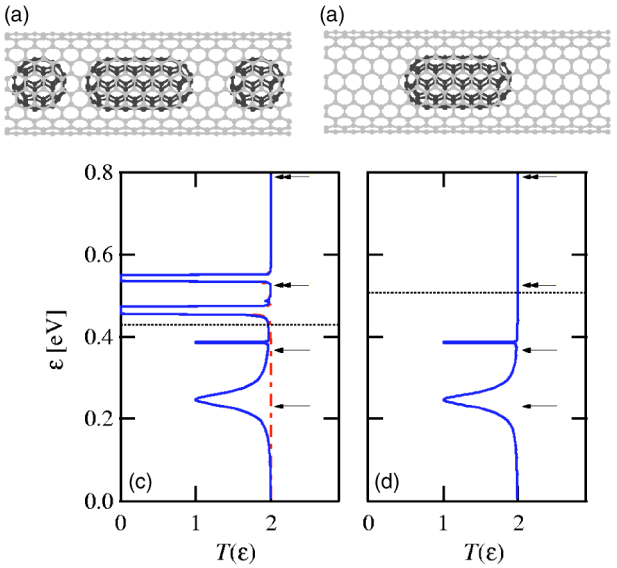

FIG. 8. (a) Atomic structure of the C_{60}@(10,10) with the (5,5) capsule. (b) Atomic structure of the (10,10) nanotube encapsulating only (5,5) capsule without C_{60}s. (c) The transmission of C_{60}@(10,10) with (5,5) capsule. Dotted-dashed lines show the transmission of C_{60}@(10,10) with ℓ_0=9.845 Å and ℓ=29.535 Å. (d) The transmission of C_{60}@(10,10) encapsulating only (5,5) capsule without C_{60}. Arrows show energy levels of the (5,5) capsule. Dotted lines show the Fermi energies of electrodes.

dips around some of the energy levels of the (5,5) capsule, that is, 0.525 and 0.789 eV. This is because these states of the (5,5) capsule do not interact with the (10,10) nanotube states due to symmetric reasons. Except this, the C_{60}@(10,10) with the (5,5) capsule exhibits qualitatively the same features as the C_{60}@(10,10) with including the C_{60} dimer or the peanut. The dip structures are the same as those of the (10,10) nanotube encapsulating only the (5,5) capsule without C_{60}s [Fig. 8(b)], which is shown in Fig. 8(d). The dip around 0.231 eV has a broad width and $T(\varepsilon)\sim 1$ at the bottom of the dip. This indicates that the electronic state of the (5,5) capsule at 0.231 eV strongly interacts with the (10,10) nanotube states, whereas the other (5,5) capsule states do weakly.

In the above C_{60}@(10,10) system with the (5,5) capsule, the (5,5) capsule merely acts as a scattering impurity center introduced in the nonperiodic C_{60}@(10,10) without the (5,5) capsule. As a result, the transmission of the former system does not exceed 2, that is, the maximum value of the transmission of the latter system. Here, we consider the system where the distance between the (5,5) capsule and the right-side C_{60} (the left-side C_{60}) is 3.248 Å (3.278 Å) and all C_{60}s are located at positions commensurate with the (10,10) nanotube, as shown in Fig. 9(a). In this system, the (5,5) capsule interacts with both the left and the right C_{60}s. Figure 9(c) shows the transmission $T(\varepsilon)$ of this C_{60}@(10,10) system with the (5,5) capsule and the energy levels of the (5,5) capsule. It is found that the transmission is larger than 2 in the energy range of 0.43–0.57 eV except around 0.46 and 0.54 eV, although the transmission at the Fermi energy ε_F of 0.43 eV, $T(\varepsilon_F)$, equals $\sim$2. This additional transmission arises from the molecular array formed by the encapsulated molecules in this system [Fig. 9(b)]. The molecular array itself exhibits considerable transmission at the energy range of 0.43–0.57 eV, as shown in Fig. 9(d). The transmission properties of the molecular array are qualitatively understood by a simple model in Appendix B. Namely, the transmission exists at the energy range where the t_{1u} state of C_{60} exists in the electrode, and has a peak around 0.525 eV which corresponds to the energy levels of the (5,5) capsule. In this way, the encapsulated (5,5) capsule not only scatters electrons but also transmits electrons if it interacts with neighboring encapsulated C_{60}s. This situation is similar to the transport in the periodic C_{60}@(10,10) with ℓ_0=9.843 Å.

IV. SUMMARY

We have studied the transport properties of various C_{60}@(10,10) systems using the realistic tight-binding model and the Green function approach. These peapod systems exhibit the following transmission properties: (1) The periodic systems exhibit the quantized transmission reflecting their band structures. In the system with ℓ_0=9.843 Å, both the (10,10) nanotube and the C_{60} array make contributions to the transmission at the Fermi energy, whereas only the (10,10) nanotube makes contributions in the system with a larger ℓ_0. (2) The transmissions of the C_{60}@(10,10) with ℓ_0=9.843 Å and $\ell>10.64$ Å are independent of the intermolecular spacing ℓ, since there is the interaction between C_{60} in the electrodes. (3) The encapsulated C_{120} molecule such as C_{60} dimer, peanut and (5,5) capsule induces dip structures in the transmission around its energy levels. The

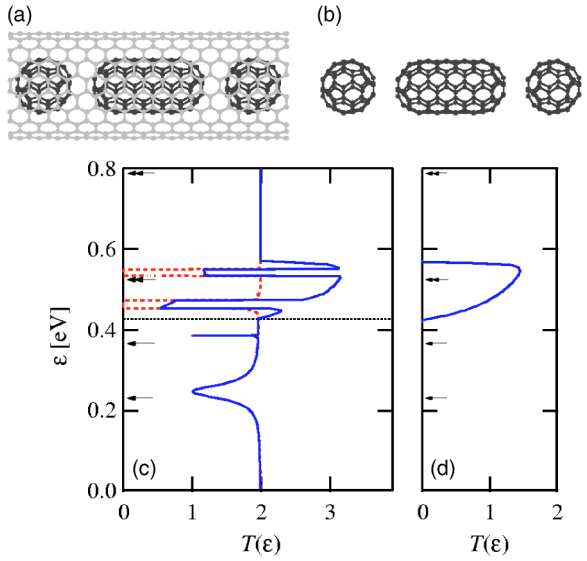

FIG. 9. (a) Atomic structure of the C_{60}@(10,10) with a (5,5) capsule. In this C_{60}@(10,10) with a (5,5) capsule, the distance between the (5,5) capsule and the right-side C_{60} is 3.248 Å (b) Atomic structure for the molecular array which has periodic C_{60}s in the electrode and a (5,5) capsule in the central region. [The same atomic structure is shown in (a) without the (10,10) nanotube.] (c) The transmission of the C_{60}@(10,10) encapsulating (5,5) capsule in the central region. Solid line (dashed line) shows the result where the distance between the (5,5) capsule and C_{60}s is 3.248 Å (5.740 Å). (d) The transmission of the molecular array which has periodic C_{60}s in the electrode and a (5,5) capsule in the central region. Arrows and dotted line show energy levels of the (5,5) capsule and Fermi energy of electrode, respectively.

strength of the interaction between C_{120} molecule and (10,10) nanotube affects the half width of the dip. (4) Although fullerenes such as C_{60} and (5,5) capsule encapsulated in the nanotube basically behave as scattering impurity centers, if there are interactions between them, the encapsulated fullerenes make contributions to the transmission.

The present results have revealed the interesting transport properties of carbon nanotubes encapsulating fullerenes inside and provided useful information for future application of carbon nanotubes to electronic nano-devices.

ACKNOWLEDGMENTS

We would like to thank N. Hamada, T. Nakayama, O. Sugino, M. Saitou, S. Okada, M. Itoh, J. Nara, Y. Fujimoto, Y. Asari and Y. Nakamura for helpful discussions. This study was supported by FSIS project and Special Coordination Funds of MEXT of the Japanese Government as well as ACT-JST. The present calculations were performed by using the Numerical Materials Simulator in NIMS.

APPENDIX A: ONE-DIMENSIONAL MODEL WITH ONE IMPURITY SITE

In order to understand the transmission of the peapod system with an impurity molecule, we consider a one-dimensional chain model with one impurity site expressed by the following Hamiltonian:

$$\mathcal{H} = \sum_{\langle ij \rangle} t c_i^+ c_j + (s_0 c_0^+ d + s_1 c_1^+ d + \text{h.c.}) + f d^+ d, \qquad \text{(A1)}$$

where c_i^+ and d^+ are the creation operators of the ith site in the chain and the impurity site, respectively, and t, s_0, and s_1 are the transfer integrals and f is the impurity level.

First we study the case that $s_1=0$. We choose the 0th site in the chain and the impurity site for the central region. For convenience, we assume that surface Green function $G^r_{\mathrm{L/R}}$ of the left/right region is

$$G^r_{\mathrm{L/R}}(\varepsilon) = \frac{\epsilon_0/2 - \mathrm{i}\Gamma_0/2}{t^2}, \qquad \text{(A2)}$$

where ϵ_0 and Γ_0 are a function of ε. Then the transmission of this one-dimensional chain is

$$T(\varepsilon) = \frac{(\varepsilon - f)^2 \Gamma_0^2}{[(\varepsilon - \epsilon_0)(\varepsilon - f) - s_0^2]^2 + (\varepsilon - f)^2 \Gamma_0^2}. \qquad \text{(A3)}$$

A dip appears at the impurity level, $\varepsilon = f$, and then $T(f)=0$.

Next we study the case that $s_0 \neq 0$ and $s_1 \neq 0$. In this case we choose the 0th and 1st sites in the chain and the impurity site for the central region. The transmission is calculated as

$$T(\varepsilon) = \frac{[s_0 s_1 + t(\varepsilon - f)]^2 \Gamma_0^2}{D(\varepsilon)/16} \qquad \text{(A4)}$$

with

$$D(\varepsilon) = [\{(2\varepsilon - \epsilon_0)^2 - \Gamma_0^2 - 4t^2\}\{\varepsilon - f\} - 8 s_0 s_1 t - 2(s_0^2 + s_1^2) \times (2\varepsilon - \epsilon_0)]^2 + [2(2\varepsilon - \epsilon_0)\Gamma_0(\varepsilon - f) - 2(s_0^2 + s_1^2)\Gamma_0]^2. \qquad \text{(A5)}$$

In the case of $s_0 \neq 0$ and $s_1 \neq 0$, a dip appears at $\varepsilon = f - s_0 s_1 / t$ and $T(f - s_0 s_1 / t) = 0$.

When $s_0 = s_1 = 0$, which corresponds to a one-dimensional chain with no impurity, the transmission is 1 for $-2t < \varepsilon < 2t$. From Eqs. (A3) and (A4), surface Green function is calculated as

$$t^2 G^r_{\mathrm{R/L}}(\varepsilon) = \frac{\varepsilon}{2} - \mathrm{i}\frac{\sqrt{4t^2 - \varepsilon^2}}{2}. \qquad \text{(A6)}$$

So we find that a half width of the dip in the case of $s_1=0$ is s_0^2/Γ_0 for $-2t < \varepsilon < 2t$ from Eq. (A3).

In this way the impurity level defines a position of the dip structure and the transfer integral between the impurity and the site in the chain defines a half width of the dip and its energy difference from the impurity level.

In the case of $s_1=0$, we obtain the Green function in the central region for $-2t < \varepsilon < 2t$ as follows:

$$G_{\mathrm{C,imp}}(\varepsilon) = \frac{\mathrm{i}\Gamma_0}{\mathrm{i}\Gamma_0(\varepsilon - f) - s_0^2}, \qquad \text{(A7)}$$

$$G_{C,0}(\varepsilon) = \frac{\varepsilon - f}{i\Gamma_0(\varepsilon - f) - s_0^2}, \tag{A8}$$

where $G_{C,imp}(\varepsilon)$ and $G_{C,0}(\varepsilon)$ are the Green function for the impurity site and the 0th site in the chain, respectively, and we choose the 0th site in the chain and the impurity site for the central region. The imaginary part of the Green function corresponds to the density of states on the ith site: $\rho_i(\varepsilon) = -\mathrm{Im}\, G_{C,i}(\varepsilon)/\pi$. At the impurity level, $\varepsilon = f$, $\rho_{imp}(\varepsilon)$ and $\rho_0(\varepsilon)$ has peak and dip structures, respectively, and the half width of the peak and the dip is s_0^2/Γ_0. This result suggests that electrons at the one-dimensional chain are scattered by the interaction with this impurity state. As a result, the dip for the transmission appears at this impurity level.

APPENDIX B: ONE-DIMENSIONAL MODEL WITH ONE SITE AS A JUNCTION

In this Appendix, we consider a one-dimensional chain expressed by Hamiltonian

$$\mathcal{H} = \sum_{\langle ij\rangle, i\neq 0, j\neq 0} t c_i^+ c_j + (s c_{-1}^+ d + s d^+ c_1 + \mathrm{h.c.}) + f d^+ d, \tag{B1}$$

where c_i^+ and $d^+(=c_0^+)$ are the creation operator of the ith site in the chain and an impurity site (the 0th site in the chain), respectively, and t and s are the transfer integrals and f is the impurity level.

We choose the only impurity site for the central region. Then the Green function of the central region is

$$G_C(\varepsilon) = \frac{\dfrac{1}{1 - s^2/t^2}}{\varepsilon - \dfrac{f}{1 - s^2/t^2} + i\dfrac{\Gamma_0 s^2/t^2}{1 - s^2/t^2}}, \tag{B2}$$

where we used the relation in Eq. (A6), $\epsilon_0 = \varepsilon$. This result suggests that a peak of the density of states of the impurity appears at $\varepsilon = f/(1 - s^2/t^2)$ and a half width of the peak is $\Gamma_0 s^2/t^2/(1 - s^2/t^2)$.

From Eq. (B2), the transmission of this one-dimensional chain is calculated as

$$T(\varepsilon) = \frac{\dfrac{\Gamma_0^2 s^4/t^4}{(1 - s^2/t^2)^2}}{\left(\varepsilon - \dfrac{f}{1 - s^2/t^2}\right)^2 + \dfrac{\Gamma_0^2 s^4/t^4}{(1 - s^2/t^2)^2}}. \tag{B3}$$

A peak of the transmission appears at $\varepsilon = f/1 - s^2/t^2$ and then $T(f/1 - s^2/t^2) = 1$. A half width of the peak is $\Gamma_0 s^2/t^2/(1 - s^2/t^2)$. In this way, the impurity level defines the position of the peak structure and the transfer integral between the impurity site and the site in the chain define a half width of the peak and its energy difference from the impurity level. The properties of the peak of the transmission correspond with the properties of the density of states for the impurity.

[1] S. Iijima, Nature (London) **354**, 56 (1991).
[2] J. W. Mintmire, B. I. Dunlap, and C. T. White, Phys. Rev. Lett. **68**, 631 (1992).
[3] N. Hamada, S. Sawada, and A. Oshiyama, Phys. Rev. Lett. **68**, 1579 (1992).
[4] R. Saito, M. Fujita, G. Dresselhaus, and M. S Dresselhaus, Appl. Phys. Lett. **60**, 2204 (1992).
[5] T. Miyake and S. Saito, Phys. Rev. B **65**, 165419 (2002).
[6] B. W. Smith, M. Monthioux, and D. E. Luzzi, Nature (London) **396**, 323 (1998).
[7] B. W. Smith and D. E. Luzzi, Chem. Phys. Lett. **321**, 169 (2000).
[8] S. Okada, S. Saito, and A. Oshiyama, Phys. Rev. Lett. **86**, 3835 (2001).
[9] S. Okada, M. Otani, and A. Oshiyama, Phys. Rev. B **67**, 205411 (2003).
[10] D. L. Strout, R. L. Murry, C. Xu, W. C. Eckhoff, G. K. Odom, and G. E. Scuseria, Chem. Phys. Lett. **214**, 576 (1993).
[11] S. Datta, *Electronic Transport in Mesoscopic Systems* (Cambridge University Press, Cambridge, 1995).
[12] D.-H. Kim, H.-S. Sim, and K. J. Chang, Phys. Rev. B **64**, 115409 (2001); **67**, 129903(E) (2003).
[13] A. Rochefort, Phys. Rev. B **67**, 115401 (2003).
[14] S. Okada and S. Saito, J. Phys. Soc. Jpn. **64**, 2100 (1995).
[15] N. Hamada, M. Yamaji, S. Okada, and S. Saito, in *Proceedings of the International Symposium on Nanonetwork Materials: Fullerenes, Nanotubes, and Related Sysytems*, Kamakura, Japan, 2001, edited by S. Saito *et al.* (American Institute of Physics, New York, 2001), p. 201.
[16] M. P. López Sancho, J. M. López Sancho, and J. Rubio, J. Phys. F: Met. Phys. **14**, 1205 (1984); **15**, 951 (1985).
[17] R. C. Haddon, L. E. Brus, and K. Raghavachari, Chem. Phys. Lett. **125**, 459 (1996).
[18] S. Saito and A. Oshiyama, Phys. Rev. Lett. **66**, 2637 (1991).
[19] E. Manousakis, Phys. Rev. B **44**, 10 991 (1991).
[20] Y.-G. Yoon, M. S. C. Mazzoni, and S. G. Louie, Appl. Phys. Lett. **83**, 5217 (2003).